

Charge state control in single InAs/GaAs quantum dots by external electric and magnetic fields

Jing Tang,^{1,2} Shuo Cao,² Yunan Gao,² Yue Sun,² Weidong Geng,^{1,*} David A. Williams,³ Kuijuan Jin,² and Xiulai Xu^{2,†}

¹*Institute of Photo-electronic Thin Film Devices and Technology, Nankai University, Tianjin, 300071, China*

²*Beijing National Laboratory for Condensed Matter Physics, Institute of Physics, Chinese Academy of Sciences, Beijing, 100190, China*

³*Hitachi Cambridge Laboratory, Cavendish Laboratory, Cambridge CB3 0HE, United Kingdom*

(Dated: July 30, 2021)

Abstract

We report a photoluminescence (PL) spectroscopy study of charge state control in single self-assembled InAs/GaAs quantum dots by applying electric and/or magnetic fields at 4.2 K. Neutral and charged exciton complexes were observed under applied bias voltages from -0.5 V to 0.5 V by controlling the carrier tunneling. The highly negatively charged exciton emission becomes stronger with increasing pumping power, arising from the fact that electrons have a smaller effective mass than holes and are more easily captured by the quantum dots. The integrated PL intensity of negatively charged excitons is affected significantly by a magnetic field applied along the sample growth axis. This observation is explained by a reduction in the electron drift velocity caused by an applied magnetic field, which increases the probability of non-resonantly excited electrons being trapped by localized potentials at the wetting layer interface, and results in fewer electrons distributed in the quantum dots. The hole drift velocity is also affected by the magnetic field, but it is much weaker.

PACS numbers: 73.21.La, 78.55.Cr, 78.67.Hc, 71.35.Ji

*Electronic address: gengwd@nankai.edu.cn

†Electronic address: xlxu@iphy.ac.cn

Self-assembled InAs/GaAs quantum dots (QDs) have been investigated intensively to implement quantum information and quantum computation, such as, single-photon sources [1–5], exciton qubits and spin qubits [6–8], quantum logic gates [9–12], spin-photon entanglement interfaces [13–15], and quantum memories [16]. Among those investigations, single spins in single dots are of particular interest because of their relatively long coherence time at low temperature [7, 17]. To achieve single charge or spin states, a precise charge control with certain spin in single quantum dots is on demand. Charges in single InAs quantum dots can be injected by resonant [18, 19] or non-resonant [20, 21] optical pumping, or by electrical pumping [3], and then they can be manipulated by applying an electric field [20, 22] or an external magnetic field [23, 24] across the quantum dots.

In an *n-i*-Schottky diode structure, the charge states of sandwiched quantum dots can be controlled precisely using external bias [21, 25–28]. For example, a quantum dot charging from +6e to -6e has been demonstrated [22] using photoluminescence (PL) spectroscopy. Using magneto-photoluminescence spectroscopy, fine-structure splitting [29], Zeeman splitting [30, 31] and diamagnetic shift [32, 33] have been investigated for different charge states in single quantum dots. Recently, coupling between triply negatively charged states and the wetting layer has also been shown using magneto-photoluminescence [34, 35]. Up to now, only a few works have been reported on the charge state control by applying an external magnetic field [23, 24]. Moskalenko and colleagues [24] reported a charge redistribution in single quantum dots with increasing magnetic field parallel to the sample growth direction (Faraday geometry), and the redistribution was explained by the reduction of electron and hole drifting velocities in the magnetic field. In this Letter, we report a comprehensive micro-PL study of the charge state control in single quantum dots with varying pumping power, applying external electric field and magnetic field. The charging states from the triply negatively charged exciton (X^{3-}) to the singly positively charged exciton (X^+) can be precisely controlled. At certain bias voltages, the intensities of the charged excitonic states can be modified with increasing magnetic field in Faraday geometry. In particular, the PL intensities of triply and doubly negatively charged excitons decrease with increasing magnetic field, while that of the singly negatively charged exciton increases.

A schematic *n-i*-Schottky structure is shown in Fig.1(a). A Si δ -doped GaAs layer with a doping density $N_d = 5 \times 10^{12} \text{ cm}^{-2}$ is used as *n* type region and contacted by annealed AuGeNi alloy. At the active regime, a semitransparent Ti with a thickness of 10 nm was

used as Schottky contact, and on top an Al mask with different apertures of 1-3 μm in diameter was patterned for addressing single quantum dots. The device was mounted on an *xyz* piezoelectric stage and placed in a helium gas exchange cryostat equipped with a superconducting magnet. The magnetic field was applied in Faraday geometry and the measurements were carried out at 4.2 K. In the micro-PL measurements, a semiconductor laser with a wavelength of 650 nm was used as pumping source and was focused on one of the apertures by a microscope objective with a large numerical aperture of 0.83. The PL from single quantum dots was collected with the same objective and dispersed through a 0.55 m spectrometer, and the spectrum was detected with a liquid nitrogen cooled charge coupled device camera with a spectral resolution of 60 μeV .

The PL measurements were firstly performed under bias voltages from -0.5 V to 0.5 V. The neutral and charged exciton complexes were observed in several individual dots with similar features. Figure 1(b) shows typical PL spectra of a single quantum dot (QD_1) as a function of bias voltage, where five discrete PL peaks can be observed. Figure 1(c) presents the spectra at three bias voltages of -0.5 V, 0 V and 0.5 V. The five emission lines in Figure 1(b) from top to bottom are assigned to the recombination from the singly positively charged exciton (X^+), the neutral exciton (X^0), the singly, doubly and triply negatively charged excitons (X^- , X^{2-} , X^{3-}), as labeled in the figure. The assignment is essentially based on the analysis of the bias voltage and the pumping power dependent PL intensities and peak positions.

With a non-resonant optical pumping, the optically generated electrons/holes relax to quantum dots via the wetting layer as shown in the Figure 1(d). The electron drift velocity is larger than that of hole because of the smaller effective mass of electron. This induces that electrons are more quickly being captured by the quantum dot than holes, resulting in that the quantum dots are more negatively charged without external field. In a Schottky diode structure as illustrated in Figure 1(d), both conduction and valence bands can be tuned with an external bias, which can be used to control the charging of the quantum dots. With a negative bias voltage, photo-generated electrons are more easily to tunnel out and leave the quantum dot positively charged, while for positive bias more photo-generated electrons are localized in quantum dots. Therefore, the PL intensities from positively charged excitons would decrease with increasing bias voltage, resulting in relatively stronger PL intensities from the negatively charged excitons. Therefore, the five peaks from left to right in Figure

1(c) are attributed to the charge states from more negative to positive in the quantum dot.

The photon energy from quantum dots is mainly determined by the electron and hole energy levels in the energy band, but it is also slightly modified by Coulomb interactions between electron-electron, electron-hole and hole-hole. Due to the Coulomb interaction, the energy of positive trion (X^+) is several meV higher than that of the neutral exciton (X^0), while the peak of negative trion (X^-) red-shifts by several meV [36]. However, X^{2-} with an additional electron to X^- only contributes a weaker Coulomb interaction, as the third electron in the quantum dot occupies the p-shell which has a smaller wave-function overlap with electrons and the hole in the s-shell. Hence, from the energy positions in QD_1, we can firmly assign that the second emission line from the top in Figure 1(b) with an energy of 1.273 eV is the neutral exciton (X^0) emission and the rest are as labeled. The binding energy between X^{2-} and X^- (X^{3-} and X^{2-}) is about 0.5 meV (1.7 meV) in this quantum dot. The coexist of the emission peaks of different charging states at certain voltages (as marked by dashed lines) is due to the thick tunneling GaAs barrier induced weak coupling between the 2DEG regime and the quantum dots, where the thickness of the barrier is 50 nm in this structure[20, 37].

The charging process in quantum dots can be further confirmed with an excitation power dependent PL mapping. Figure 2 shows the PL spectra of QD_1 as a function of bias voltage with different pumping powers. At a low pumping power of 0.06 μ W and at zero bias voltage, only a single electron and a single hole can be generated and form a neutral exciton in a time as marked in the top panel. This confirms the neutral exciton emission assignment above. The negatively charged exciton emission can only be identified with a positive bias towards 0.5 V. With increasing pumping power to 0.53 μ W and 1.46 μ W, the negatively charged exciton peaks (X^- and X^{2-}) become stronger and a negative bias voltage is required to observe X^0 and X^+ emission. With a pumping power at 2.37 μ W, the X^- and X^{2-} peak intensities are getting even stronger and X^{3-} peak appears. The negative bias voltage required to observe X^0 and X^+ peaks is out of the applied voltage range. The trend that the higher the pumping power, the more negatively charging in the quantum dots is resulted from the fact that the electrons are more easily being captured than holes due to its smaller effective mass.

In the above, we show that the charge states in the quantum dot can be controlled by applying a bias voltage, where the carrier capture process plays an important role. In

the following work, we show the charge state control by applying magnetic field. In the experiments, the excitation laser energy (1.908 eV) is higher than the energy gap of GaAs barrier (1.518 eV). Hence, the optically generated electrons and holes with certain kinetic energies will firstly emerge at GaAs matrix separately or in pairs, then relax to the wetting layer and finally be captured by the quantum dots [38]. The applied bias modifies the band structure of the devices as shown in Figure 1(d), which mainly affects the capture process along the growth direction. The laser spot size ($1\sim 2\ \mu\text{m}$ in diameter) is far larger than the dot size ($\sim 25\ \text{nm}$), the drifting of optically generated carriers in quantum dot plane cannot be avoided and provides an additional way to control the charging states of quantum dots. Applying a magnetic field perpendicular to the device plane (Faraday geometry) can affect the electron and hole in plane transport by magnetic field induced cyclotron motion [24].

Figure 3(a) shows the PL spectra under magnetic fields varied from 0 T to 9 T, and in each panel the bias voltage varies from -0.5 V to 0.5 V. All the spectral lines from different charged states (as marked on top of the figure) split with increasing magnetic field, which is due to Zeeman effect. The similar g factors for all the charged states are calculated to be about 2.5 ± 0.08 , similar to the reported values [33]. The average peak position of the splitting peaks shifts towards the high energy with increasing magnetic field, which is due to the diamagnetic shift. It can be seen that the integrated intensities of X^{3-} and X^{2-} decrease gradually with an increase of applied magnetic field, and the X^{3-} peak almost quenched with a magnetic field at 6 T, while that of X^{-} increases. In addition, the intensities of X^0 and X^+ decrease slightly with increasing magnetic field.

For clarity, Figure 3(b) shows the PL spectra in the negatively charged exciton regime as a function of magnetic field with bias voltages at -0.5 V, 0 V and +0.5 V. In each panel, the PL intensity of X^{-} increases with increasing magnetic field, while the PL intensities of X^{2-} and X^{3-} decrease. To obtain a clear intensity variation induced by the applied magnetic field, the integrated intensities of the negatively charged excitons for each branch of the Zeeman splitting (σ^+ and σ^-) are plotted in Figure 3(c) at three bias voltages. At zero magnetic field with a bias voltage at -0.5 V, only X^{-} and X^{2-} can be observed with relatively low intensities, and the X^{-} and X^{2-} are getting stronger and X^{3-} appears at bias voltages of 0 V and 0.5 V. At 0.5 V, the intensities of X^{2-} and X^{3-} decrease with applying magnetic field and X^{3-} intensity approaches to zero with a magnetic field up to 6 T. However, X^{-} peak is very weak at 0 T and quickly increases with a magnetic field

tuned to 4 T and then saturates. We ascribe this charging state control to that the carrier transport in quantum dot plane is modified by the magnetic field.

Due to the growth induced variations of alloy composition and strain in the quantum dot plane, localized potential fluctuations can be formed at the InAs/GaAs interfaces [39–41]. The potential fluctuations could trap the optically excited electrons and holes, and affect the carrier relaxation, which ultimately affects the PL intensities of the quantum dots [39, 42]. Owing to that the effective mass of hole ($m_h = 0.45 m_0$) is ~ 6.72 times larger than that of electrons ($m_e = 0.067 m_0$), where m_0 represents the mass of free-electron [43], holes are more easily being trapped by the localized potentials than electrons. This induces a larger probability for electrons being captured by quantum dots than holes. It could be an additional reason for that the negatively charged exciton peaks are getting stronger with increasing pumping power without applied electric and magnetic fields (as shown in Figure 2).

Moskalenko et al. [24] recently have studied the influence of the vertical magnetic field on the electron and hole transport in similar quantum dots, where they found that the PL intensity of X^0 increases while those of X^- and X^{2-} decrease with increasing magnetic field. The magnetic field applied in Faraday geometry induces the cyclotron motion of electrons and holes, which reduces their drifting velocities. The reduced drifting of electrons and holes would raise their probability of being trapped by local potential prior to arriving at the quantum dot. This model requires that $\omega_c^{e(h)} \times \tau_{sc}^{e(h)}$ is larger than one [24, 44]. Here $\omega_c^{e(h)}$ is the cyclotron frequency $e^*B/m_{e(h)}$, where e^* is the elementary charge, $\tau_{sc}^{e(h)}$ is the scattering time of an electron (hole). We used the scattering time of 3.4 ps and 0.74 ps for electrons and holes in GaAs from reference [24, 45]. To achieve $\omega_c^{e(h)} \times \tau_{sc}^{e(h)} > 1$, the minimum magnetic field needed for affecting electrons (holes) is 0.11 T (3.4 T). It indicates that electrons are much easier than holes to be affected by the magnetic field. This means that more electrons would be affected during the drifting in the quantum dot plane and trapped by the localized potentials at 4.2 K [24, 41], resulting in a reduced negatively charging in quantum dots with increasing magnetic field. Therefore the PL intensities of X^{3-} and X^{2-} decrease while that of X^- increases. The magnetic field was not strong enough to observe the intensity increases of X^0 and X^+ yet. On the contrast, a slight intensity decrease of X^0 and X^+ could be due to the increased number of holes being trapped by the localized potentials in high magnetic field.

To further examine the model and show the reproducibility of the observation, Figure 4 shows the PL spectra of another quantum dot (QD_2) as a function of magnetic field at different bias voltages. The charged exciton peaks are labeled and the dashed lines mark the Zeeman splitting. Similar features as QD_1 can be observed. At -0.5 V, X^- peak (as labeled in the Figure 4) dominates in the spectra and total intensity is relatively low. As the bias voltage increases, the X^{2-} intensity increases and dominates in the spectrum at 0 T. However, the intensity of X^{2-} quickly decreases while that of X^- increases with a magnetic field only at about 2 T, which further supports above discussion.

In conclusion, charging state control has been demonstrated in single quantum dots at 4.2 K by varying pumping power, applying an external electric field and/or a magnetic field. Because the effective mass of electron in GaAs is much less than that of hole, electrons have a larger drift velocity and a larger probability being captured by quantum dots, resulting in stronger PL intensities of negatively charged excitons with increasing the pumping power. In addition, the recombination from different charged states (from X^{3-} to X^+) can be precisely controlled by an applied electric field. With a magnetic field applied parallel to the growth direction, electron transport is more easily to be affected by the magnetic field than that of hole, because the electrons can form cyclotron orbit with a smaller magnetic field. This increases the probability of the electrons being trapped by the localized potentials in the quantum dot plane, which results in carrier redistribution in quantum dots. Our results suggest that by tuning electric field, magnetic field and pumping power, the charging states of a single quantum dot can be precisely controlled.

I. ACKNOWLEDGEMENTS

This work was supported by the National Basic Research Program of China under Grant No. 2013CB328706 and 2014CB921003; the National Natural Science Foundation of China under Grant No. 11174356 and 61275060; the Strategic Priority Research Program of the Chinese Academy of Sciences under Grant No. XDB07030200; the Hundred Talents Program of the Chinese Academy of Sciences, and the China Postdoctoral Science Foundation under Grand No. 2013M540155. We thank Andrew Ramsay, Jonathan Mar, Weidong Sheng and

Mete Atatüre for very helpful discussions.

- [1] J. Kim, O. Benson, H. Kan, and Y. Yamamoto, *Nature* **397**, 500 (1999).
- [2] P. Michler, A. Kiraz, C. Becher, W. V. Schoenfeld, P. M. Petroff, L. Zhang, E. Hu, and A. Imamoglu, *Science* **290**, 2282 (2000).
- [3] X. Xu, D. A. Williams, and J. R. A. Cleaver, *Appl. Phys. Lett.* **85**, 3238 (2004).
- [4] A. J. Bennett, D. C. Unitt, P. See, A. J. Shields, P. Atkinson, K. Cooper, and D. A. Ritchie, *Appl. Phys. Lett.* **86**, 181102 (2005).
- [5] X. Xu, I. Toft, R. T. Phillips, J. Mar, K. Hammura, and D. A. Williams, *Appl. Phys. Lett.* **90**, 061103 (2007).
- [6] R. S. Kolodka, A. J. Ramsay, J. Skiba-Szymanska, P. W. Fry, H. Y. Liu, A. M. Fox, and M. S. Skolnick, *Phys. Rev. B* **75**, 193306 (2007).
- [7] K. M. Weiss, J. Miguel-Sanchez, and J. M. Elzerman, *Sci. Rep.* **3** (2013).
- [8] A. Zrenner, E. Beham, S. Stuffer, F. Findeis, M. Bichler, and G. Abstreiter, *Nature* **418**, 612 (2002).
- [9] N. H. Bonadeo, J. Erland, D. Gammon, D. Park, D. S. Katzer, and D. G. Steel, *Science* **282**, 1473 (1998).
- [10] F. Troiani, U. Hohenester, and E. Molinari, *Phys. Rev. B* **62**, R2263 (2000).
- [11] L. Besombes, J. J. Baumberg, and J. Motohisa, *Phys. Rev. Lett.* **90**, 257402 (2003).
- [12] J. Fei, D. Zhou, Y.-P. Shim, S. Oh, X. Hu, and M. Friesen, *Phys. Rev. A* **86**, 062328 (2012).
- [13] K. De Greve, L. Yu, P. L. McMahon, J. S. Pelc, C. M. Natarajan, N. Y. Kim, E. Abe, S. Maier, C. Schneider, M. Kamp, et al., *Nature* **491**, 421 (2012).
- [14] J. R. Schaibley, A. P. Burgers, G. A. McCracken, L.-M. Duan, P. R. Berman, D. G. Steel, A. S. Bracker, D. Gammon, and L. J. Sham, *Phys. Rev. Lett.* **110**, 167401 (2013).
- [15] L. Webster, K. Truex, L.-M. Duan, D. Steel, A. Bracker, D. Gammon, and L. Sham, *Phys. Rev. Lett.* **112**, 126801 (2014).
- [16] T. Lundstrom, W. Schoenfeld, H. Lee, and P. M. Petroff, *Science* **286**, 2312 (1999).
- [17] R. J. Warburton, *Nat. Mater.* **12**, 483 (2013).
- [18] M. Atatüre, J. Dreiser, A. Badolato, and A. Imamoglu, *Nat. Phys.* **3**, 101 (2007).
- [19] Y.-M. He, Y. He, Y.-J. Wei, D. Wu, M. Atatüre, C. Schneider, S. Höfling, M. Kamp, C.-Y.

- Lu, and J.-W. Pan, *Nat. Nanotechnol.* **8**, 213 (2013).
- [20] J. D. Mar, X. L. Xu, J. J. Baumberg, F. S. F. Brossard, A. C. Irvine, C. Stanley, and D. A. Williams, *Phys. Rev. B* **83**, 075306 (2011).
- [21] M. Ediger, P. A. Dalgarno, J. M. Smith, B. D. Gerardot, R. J. Warburton, K. Karrai, and P. M. Petroff, *Appl. Phys. Lett.* **86**, 221909 (2005).
- [22] M. Ediger, G. Bester, A. Badolato, P. M. Petroff, K. Karrai, A. Zunger, and R. J. Warburton, *Nat. Phys.* **3**, 774 (2007).
- [23] E. S. Moskalenko, L. A. Larsson, M. Larsson, P. O. Holtz, W. V. Schoenfeld, and P. M. Petroff, *Nano Lett.* **9**, 353 (2009).
- [24] E. S. Moskalenko, L. A. Larsson, M. Larsson, P. O. Holtz, W. V. Schoenfeld, and P. M. Petroff, *Phys. Rev. B* **78**, 075306 (2008).
- [25] J. D. Mar, X. L. Xu, J. J. Baumberg, A. C. Irvine, C. Stanley, and D. A. Williams, *Appl. Phys. Lett.* **99**, 031102 (2011).
- [26] J. D. Mar, X. L. Xu, J. J. Baumberg, A. C. Irvine, C. Stanley, and D. A. Williams, *J. Appl. Phys.* **110**, 053110 (2011).
- [27] M. Baier, F. Findeis, A. Zrenner, M. Bichler, and G. Abstreiter, *Phys. Rev. B* **64**, 195326 (2001).
- [28] A. S. Bracker, E. A. Stinaff, D. Gammon, M. E. Ware, J. G. Tischler, A. Shabaev, A. L. Efros, D. Park, D. Gershoni, V. L. Korenev, et al., *Phys. Rev. Lett.* **94**, 047402 (2005).
- [29] M. Bayer, G. Ortner, O. Stern, A. Kuther, A. A. Gorbunov, A. Forchel, P. Hawrylak, S. Fafard, K. Hinzer, T. L. Reinecke, et al., *Phys. Rev. B* **65**, 195315 (2002).
- [30] I. Toft and R. T. Phillips, *Phys. Rev. B* **76**, 033301 (2007).
- [31] A. Högele, M. Kroner, S. Seidl, K. Karrai, M. Atatüre, J. Dreiser, A. Imamoğlu, R. J. Warburton, A. Badolato, B. D. Gerardot, et al., *Appl. Phys. Lett.* **86**, 221905 (2005).
- [32] C. Schulhauser, D. Haft, R. J. Warburton, K. Karrai, A. O. Govorov, A. V. Kalameitsev, A. Chaplik, W. Schoenfeld, J. M. Garcia, and P. M. Petroff, *Phys. Rev. B* **66**, 193303 (2002).
- [33] M.-F. Tsai, H. Lin, C.-H. Lin, S.-D. Lin, S.-Y. Wang, M.-C. Lo, S.-J. Cheng, M.-C. Lee, and W.-H. Chang, *Phys. Rev. Lett.* **101**, 267402 (2008).
- [34] B. Van Hattem, P. Corfdir, P. Brereton, P. Pearce, A. M. Graham, M. J. Stanley, M. Hugues, M. Hopkinson, and R. T. Phillips, *Phys. Rev. B* **87**, 205308 (2013).
- [35] K. Karrai, R. J. Warburton, C. Schulhauser, A. Högele, B. Urbaszek, E. J. McGhee, A. O.

- Govorov, J. M. Garcia, B. D. Gerardot, and P. M. Petroff, *Nature* **427**, 135 (2004).
- [36] R. J. Warburton, B. T. Miller, C. S. Dürr, C. Bödefeld, K. Karrai, J. P. Kotthaus, G. Medeiros-Ribeiro, P. M. Petroff, and S. Huant, *Phys. Rev. B* **58**, 16221 (1998).
- [37] N. A. J. M. Kleemans, J. van Bree, A. O. Govorov, J. G. Keizer, G. J. Hamhuis, R. Nötzel, A. Y. Silov, and P. M. Koenraad, *Nat. Phys.* **6**, 534 (2010).
- [38] P. W. Fry, J. J. Finley, L. R. Wilson, A. Lemaître, D. J. Mowbray, M. S. Skolnick, M. Hopkinson, G. Hill, and J. C. Clark, *Appl. Phys. Lett.* **77**, 4344 (2000).
- [39] C. Lobo, R. Leon, S. Marcinkevičius, W. Yang, P. C. Sercel, X. Z. Liao, J. Zou, and D. J. H. Cockayne, *Phys. Rev. B* **60**, 16647 (1999).
- [40] T. J. Krzyzewski, P. B. Joyce, G. R. Bell, and T. S. Jones, *Phys. Rev. B* **66**, 121307 (2002).
- [41] S. Cao, X. Ji, K. Qiu, Y. Gao, Y. Zhao, J. Tang, Z. Xu, K. Jin, and X. Xu, *Semicond. Sci. Technol.* **28**, 125004 (2013).
- [42] Y. Toda, O. Moriwaki, M. Nishioka, and Y. Arakawa, *Phys. Rev. Lett.* **82**, 4114 (1999).
- [43] H. Hillmer, A. Forchel, S. Hansmann, M. Morohashi, E. Lopez, H. P. Meier, and K. Ploog, *Phys. Rev. B* **39**, 10901 (1989).
- [44] C. Kittel, *Introduction to Solid State Physics* (Wiley, New York, 1976), 5th ed.
- [45] U. Bockelmann, G. Abstreiter, G. Weimann, and W. Schlapp, *Phys. Rev. B* **41**, 7864 (1990).

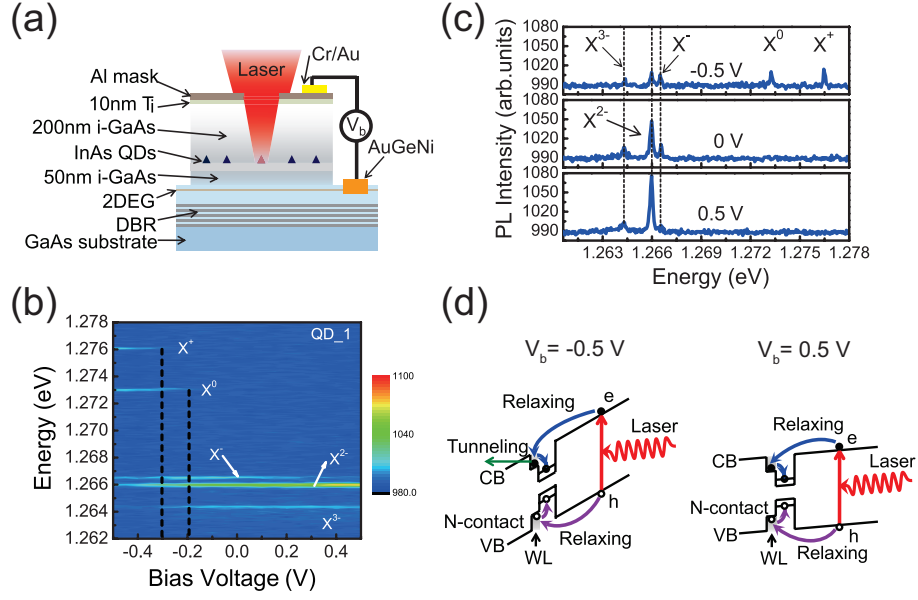


FIG. 1: (a) A schematic diagram of a n - i -Schottky device. (b) PL spectra with bias voltages sweeping from -0.5 V to $+0.5$ V of QD₁ with an excitation power of $2.37 \mu\text{W}$. The PL peaks from X^{3-} , X^{2-} , X^- , X^0 and X^+ are labeled in the figure. The dotted lines mark the beginning of emission lines of X^0 and X^+ . (c) PL spectra with bias voltages at -0.5 V, 0 V and $+0.5$ V from the top to the bottom panels. (d) Band profiles of the n - i -Schottky diode structure under bias voltages of -0.5 V and $+0.5$ V.

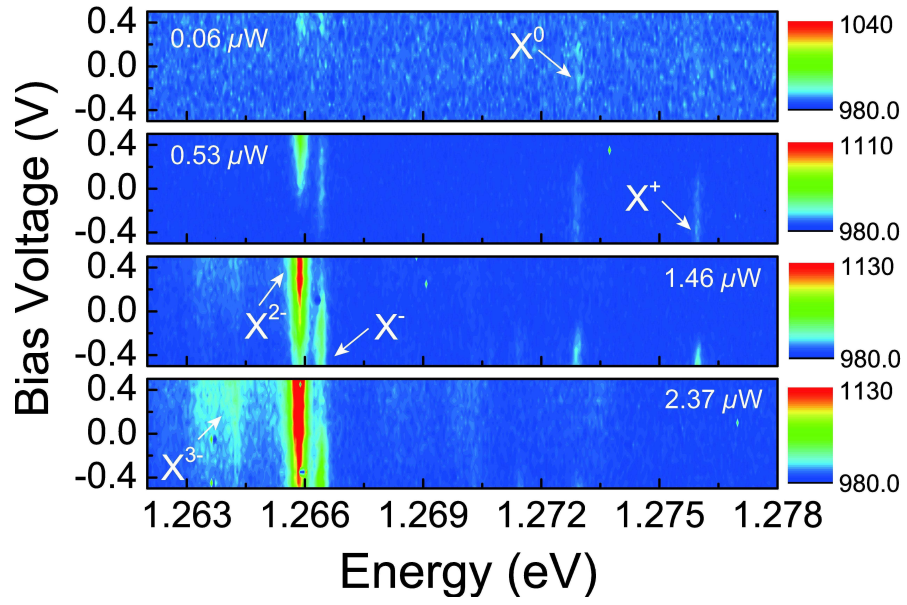


FIG. 2: PL spectra of QD_1 as a function of bias voltage from -0.5 V to +0.5 V with different pumping powers. The pumping powers from the top panel to the bottom panel are 0.06 μW , 0.53 μW , 1.46 μW and 2.37 μW , respectively.

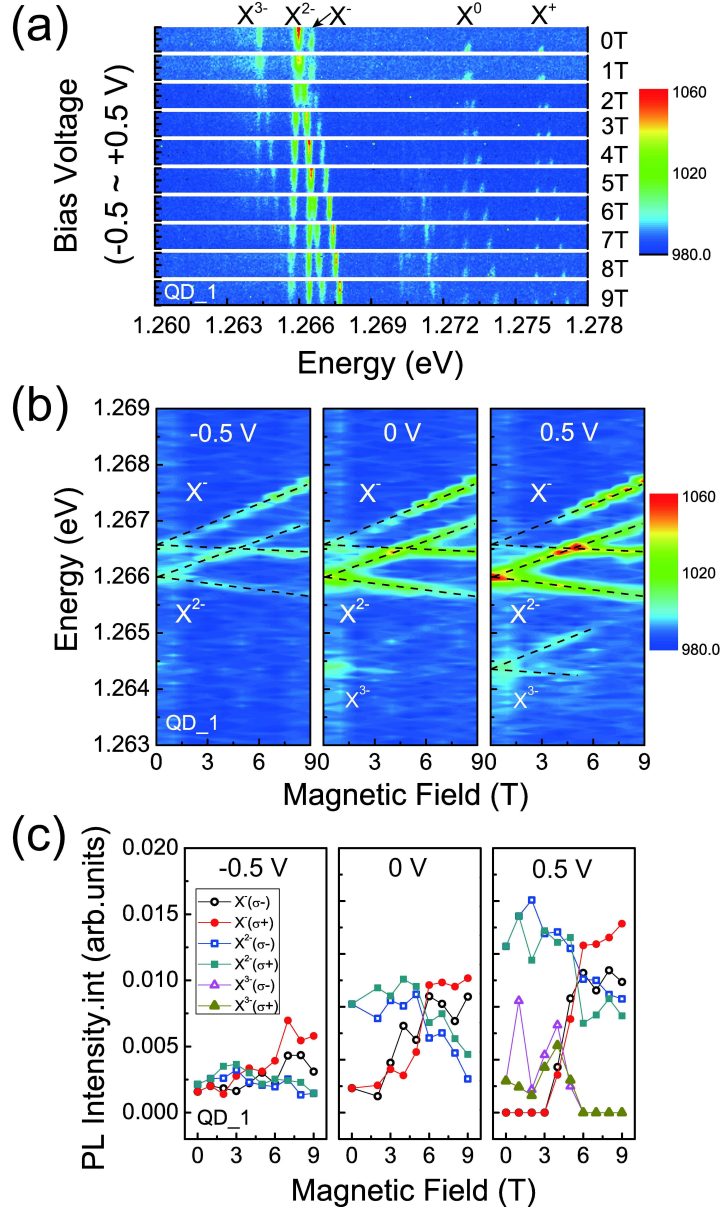


FIG. 3: (a) Contour plot of the PL spectra of QD_1 as a function of bias voltage from -0.5 V to +0.5 V with different magnetic fields from 0 T to 9 T in Faraday geometry. Each panel shows PL spectra of QD_1 as a function of bias voltage from -0.5 V (bottom) to +0.5 V (top). (b) PL spectra of X^- , X^{2-} and X^{3-} in QD_1 as a function of applied magnetic field from 0 T to 9 T with bias voltage at -0.5 V, 0 V and +0.5 V, respectively. The dashed lines mark the corresponding energy levels by the Zeeman splitting. (c) The integrated intensities of X^- , X^{2-} and X^{3-} as a function of the applied magnetic field at different bias voltages.

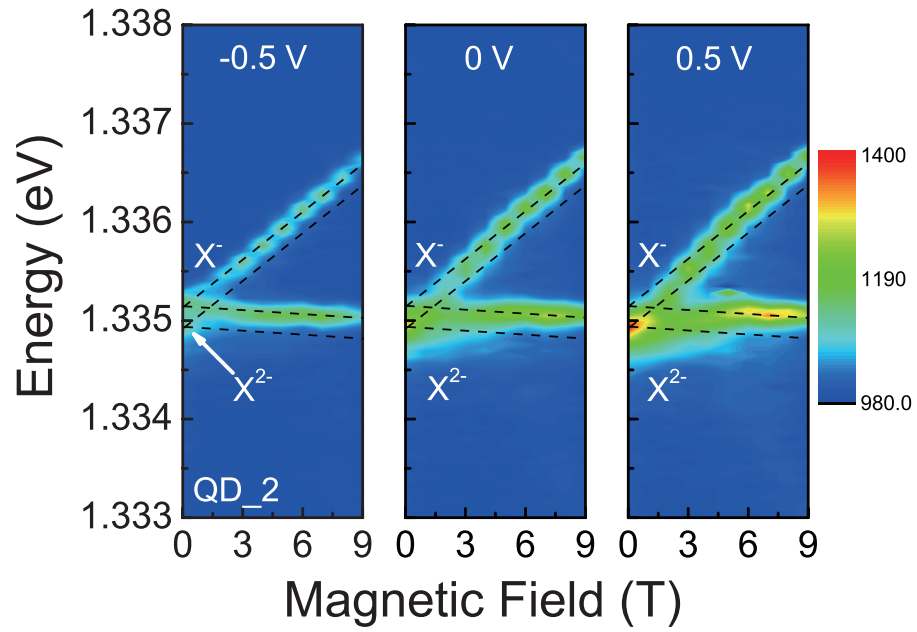


FIG. 4: PL spectra of X^{2-} and X^{-} from QD_2 as a function of applied magnetic field from 0 T to 9 T, with bias voltages at -0.5 V, 0 V and +0.5 V. The dashed lines mark the corresponding energy levels by the Zeeman splitting for different charge states.